Journal:	*Optics Letters*
Article Title:	Extreme local field enhancement by hybrid epsilon-near-zero–plasmon mode in thin films of transparent conductive oxides
Authors:	Innem V. A. K. Reddy, Josep M. Jornet, Alexander Baev, and Paras N. Prasad
Accepted for publication:	14 September 2020
Final version published:	12 October 2020
DOI:	https://doi.org/10.1364/OL.402647

Extreme Local Field Enhancement by Hybrid Epsilon-near-zero/Plasmon Mode in Thin Films of Transparent Conductive Oxides

INNEM V.A.K REDDY[1,2,3], JOSEP M. JORNET[4], ALEXANDER BAEV[1], AND PARAS N. PRASAD[1,*]

[1] The Institute for Lasers, Photonics and Biophotonics, University at Buffalo, Buffalo, NY 14260-3000, USA
[2] Department of Electrical Engineering, University at Buffalo SUNY, NY 14260
[3] Biological and Environmental Science Engineering Division, King Abdullah University of Science and Technology, Thuwal, 23955, Saudi Arabia
[4] Department of Electrical and Computer Engineering, Northeastern University, Boston, MA 02115
[*] Corresponding author: pnprasad@buffalo.edu

Compiled September 6, 2020

Epsilon-near-zero (ENZ) materials display unique properties, among them large local field enhancement at ENZ frequency is of particular interest for many potential applications. In this paper, we introduce a concept that a combination of epsilon-near-zero- and surface plasmon-polariton modes can be excited over an interface between a dielectric and a single ENZ layer in a specific frequency region which can lead to extreme enhancement of local electric field. We demonstrate it by a systematic numerical simulation using finite element analysis and consider two configurations (Kretschmann configuration and a grating configuration), where an indium tin oxide (ITO) layer is sandwiched between two dielectric slabs. We confirm the formation of a hybrid mode at the ITO/dielectric interface at the wavelength of ENZ, as the ITO layer thickness reduces. The hybrid mode provides both high confinement and long propagation distance, which makes it more attractive for many applications than just a pure ENZ mode.

http://dx.doi.org/10.1364/ao.XX.XXXXXX

In the recent decade, there has been a significant interest in the epsilon-near-zero and negative refractive index (meta) materials, due to their unique optical properties, that led to the whole new sub-field of photonics - metaphotonics [1], and due to their potential applications [2]. In ENZ materials, the real part of dielectric permittivity approaches zero at a specific frequency, and the electric and magnetic fields decouple at this point. Therefore, ENZ materials exhibit some unique properties at these frequencies. Some examples of naturally occurring ENZ materials are transparent conducting oxides (TCOs), such as indium tin oxide (ITO) or doped cadmium oxide (CdO). Furthermore, novel metamaterials can be engineered to exhibit ENZ-like behavior as well. Some of the prominent applications with ENZ materials include extreme non-linearities [3, 4], meta-lensing [5], and highly directional emission [6]. There have been quite a few studies on ENZ materials and their corresponding electromagnetic modes at the interface with dielectrics. In 2012, Vassant et al. [7] put forth the concept of an ENZ/Surface Phonon Polariton mode (ENZ SPhP mode) that was observed in a GaAs quantum well. They combined ENZ enhancement observed in GaAs, along with the excitation of surface phonon-polaritons to generate efficient broadband absorption. The SPhP mode was excited with the help of a gold grating fabricated over a AlGaAs/GaAs/AlGaAs quantum well. This combination of ENZ and SPhP modes has been referred to as the ENZ mode. Later in the year, the same group studied a leaky mode in thin dielectric films and their field enhancement, leading to the conceptualization of Berreman ENZ mode [8–10]. The configuration used here had a dielectric layer over the metal, and their combined permittivity approached zero, leading to extreme field enhancement. In this work, the authors showed that the dispersion of an ENZ mode assumes a flat line, as the thickness of the dielectric film reduces. Shortly after, Campione et al. [11] discussed extreme field enhancement in subwavelength ENZ slabs, when excited by TM polarized light. As the thickness of the slabs reduces, it was shown that a long-range plasmon (LRP) mode would morph into an ENZ mode [12]. The concept of LRPs is often interlinked with the ENZ mode. Economou [13] first predicted the splitting of surface plasmon-polariton (SPP) mode into a long-range plasmon (LRP) and a short-range plasmon (SRP) in a thin metal film, and studied their dispersion. He introduced the concept of short- and long-range polaritons, and explained how the dispersion of LRP approaches the plasma frequency, as the film thickness reduces. A similar behavior is observed in thin ENZ slabs, where the dispersion of the LRP mode becomes flat as the thickness reduces and takes the form of an ENZ mode. Preliminary experiments on doped semiconductor layers confirmed the existence of the ENZ mode [14]. Taliercio et al. [15] used a configuration of thin dielectric slabs over metals, which was similar to that reported by Vassant et al. [8], and proposed the existence of Brewster mode. This mode is identical to the Berreman ENZ mode with a strong resonant absorption peak [16, 17]. Further studies on engineered ENZ metamaterials revealed a quasi-confined ENZ mode [18], where one can observe high field

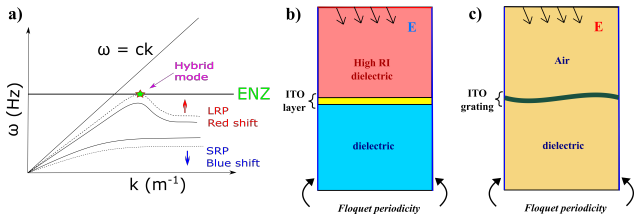

Fig. 1. (a) Dispersion curves of SPR and ENZ. A hybrid mode shown in the figure is where both ENZ and SPR modes co-exist, (b) An ITO layer sandwiched between a high RI and a dielectric. The EM field is incident from a periodic port and the Floquet periodicity is used on the edges, (c) Similar domain as (b) except that the layer is in the form of a sinusoidal grating and has air as in the incident medium.

enhancement even in thick slabs, unlike the previous assumption of ENZ modes occurring only in thin slabs. Later in the year, Runnerstrom et al. [19] demonstrated a polaritonic hybrid ENZ mode in doped CdO bi-layers. This engineered combination takes the best of both worlds and offers large field confinement, along with a substantial propagation length. All these years, the definition of ENZ mode expanded, while the core idea of flat line dispersion and extreme field enhancement remained the same. Engineered ENZ metamaterials gained popularity and generated a great deal of interest [20–22]. Many applications [23–25] were put forth by several groups, which included enhanced second-harmonic generation, extreme non-linearities, and vastly enhanced light-matter interactions in general.

In this paper, we propose the concept of a hybrid mode which is a combination of ENZ and surface plasmon-polariton (SPP) modes in the same material. This hybrid mode is not similar to the ENZ-SphP mode [7] or hybrid polaritonic ENZ mode [19] as published before. We show that this hybrid mode can be generated in the same material and does not require external gratings or bi-layers of doped oxides to excite the plasmons. When an ENZ material is sandwiched between two dielectrics, it will exhibit ENZ field enhancement at the ENZ wavelength and surface plasmon resonance (SPR) field enhancement at a longer wavelength. These two enhancement regimes can be brought together by shifting the SPP mode towards the ENZ wavelength. The existence of super modes [13, 26] and the possibility of a split in the dispersion curve in a thin conducting film, allows the shift of the LRP SPP mode, and under the right conditions one can observe both modes converge and produce significantly larger field enhancement than either one of them separately. To demonstrate this concept, we chose indium tin oxide (ITO), a transparent conducting metal oxide, whose permittivity crosses zero at 1237 nm. ITO has been studied previously for exciting SPPs [27] as well as for the ENZ mode [14], but never involving both the modes at the same time. Other transparent conducting oxides such as doped CdO, TiN and Al:ZnO can also be used in the place of ITO. For the first time, we illustrate this phenomenon in conductive ENZ materials and discuss the configurations along with the field enhancement plots.

Indium tin oxide (ITO) is a naturally occurring ENZ material, with the real part of its relative permittivity crossing zero at 1237 nm. In this study, we focus our attention on ITO/dielectric interface, and explore ways by which we can further boost the local electric field enhancement (FE). We demonstrate, for the first time, the possibility to obtain a hybrid mode at the ITO/dielectric interface. We perform a theoretical analysis by building parametric models, and illustrate configurations at which a hybrid mode exists. The boundary conditions for a TM-polarized wave at a dielectric/ENZ material interface are given by:

$$E_{x,incident} = E_{x,ENZ} \quad and \quad E_{y,ENZ} = \frac{\varepsilon_{dielectric}}{\varepsilon_{ENZ}} E_{y,incident} \qquad (1)$$

Here, the tangential x-component of the electric field remains continuous across the interface. The normal y-component, however, experiences discontinuity, as it is inversely proportional to the permittivity of the ENZ material. As discussed before, for a lossless ENZ material, the value of permittivity can reach zero at the ENZ frequency, which leads to giant field enhancement. Here, the field enhancement is expressed as the ratio of the square of the electric field inside the ENZ material to that of the incident field. Although the real part of epsilon reaches zero at the ENZ frequency, the non-zero imaginary part restricts the FE to a finite value. For an ENZ material like ITO, it is possible to excite an ENZ mode. The dispersion curve of ENZ mode is almost flat, and one can excite this mode with or without momentum matching conditions. In other words, a high refractive index medium (prism coupler) on top of the ITO layer may not be needed. On the other hand, since ITO exhibits a metallic, Drude-type behavior, it is also possible to excite a Surface Plasmon Polariton (SPP) mode. The real part of ITO permittivity becomes negative at longer wavelengths with respect to the ENZ wavelength, and hence, the SPP mode should be located at longer wavelengths or lower frequencies. As we reduce the thickness of ITO, the SPP mode splits due to the interaction of modes between the top and the bottom dielectric layers. This hybridization process results in the splitting of a long-range plasmon (LRP) mode anda short-range plasmon (SRP) mode. These modes move apart as the thickness reduces, and at some point, the dispersion curve of the LRP mode meets the practically flat dispersion curve of the ENZ mode (as shown in Figure 1(a)). At this intersection point, we can see that both the ENZ mode and the LRP mode coexist, hence forming a hybrid mode. Therefore, under the right conditions, one can excite this hybrid mode on ITO-dielectric interfaces, thus yielding extreme field enhancement.

We carried out numerical analysis by building 2D models in COMSOL, a finite element analysis software [28]. The computational domain is a simple three-layer system, with an ITO layer sandwiched between two different dielectric layers. Figures 1(b,c) display this domain used for calculations. The electric field is incident via the periodic port condition, and the Floquet periodicity condition to the edges is imposed to mimic semi-infinite layers. As shown in Figs. 1(b) and 1(c), we chose two configurations: a) a plain ITO-layer sandwiched between the dielectric layers with a high refractive index (RI) contrast, and b) an ITO grating on a dielectric material with air as the incident medium. The first arrangement mimics the Kretschmann configuration, which requires a high RI incident medium for momentum matching. Here, we used an incident medium with a RI of 5. However, transparent high RI materials are rare (some transition metal dichalcogenides, TMDs, can have rather high RI) [29, 30], and it is challenging to implement it experimentally. For this purpose, we came up with a grating configuration with air as an incident medium (Fig. 1(c)). Here, diffraction over the grating assists with the momentum matching. We collect the field enhancement values in both the arrangements and moni-

tor the variation while varying the crucial parameters like the thickness, the angle of incidence, the wavelength, the period of the grating, and the RI of the substrate. Our results are presented in 2D contour plots of the FE with respect to the change in wavelength and the angle of incidence.

A. Configuration 1

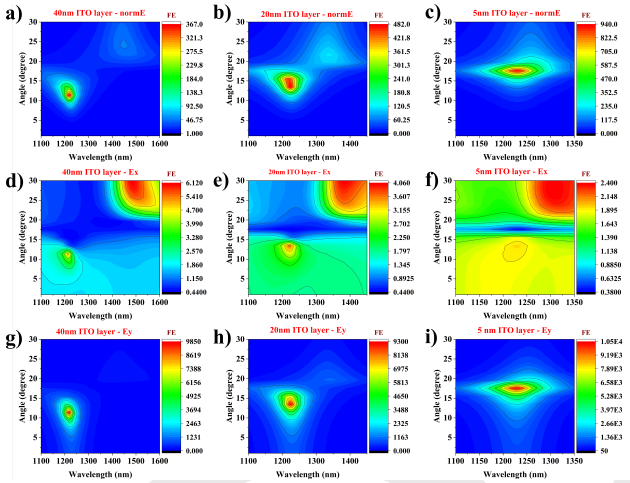

Fig. 2. Field enhancement (FE) plots vs, wavelength and the angle, observed in the configuration 1 by varying the thickness of ITO layer deposited on a dielectric of RI 1.5 (a-c) Electric field norm, (d-f) x-component of the field, and (g-i) y-component of the field.

Fig. 2 summarizes the FE plots we observed by varying the thickness of the ITO layer. Figs. 2(a-c) display the electric field norm, Fig. 2(d-f) show the tangential component of the field, and Fig. 2(g-i) - the normal to the interface component of the field. Figs. 2(a,d,g) show two distinct localized regions, one located close to the ENZ wavelength (1235 nm) while the other at 1450 nm, at different angles of incidence. The hotspot near ENZ wavelength is due to the ENZ mode, while the spot at 1450 nm corresponds to the SPR enhancement. As the thickness reduces, we see that these hotspots merge, leading to a hybrid mode. However, the ENZ related enhancement stays at the same location in terms of wavelength and the angle of incidence. This behavior correlates with the fact that the ENZ mode has a flat dispersion. At the same time, SPR related enhancement shifts towards the ENZ wavelength, confirming the hypothesis of dispersion curve (LRP) moving up and intersecting the ENZ curve at some point. As the dispersion curve of plasmon-polariton migrates towards the plasma frequency, the wavelength at which we excite plasmons reduces. In addition, the angle gradually shifts towards the ENZ hotspot, further affirming that, as the curves intersect, we can excite a combination of modes at the same wavelength and angle of incidence. We can observe the shift in wavelength and the angle of incidence in the plots 2(b,c), (e,f), and (h,i) as the thickness reduces. For the Ey field, the FE value increases from 9850 to 10500 at the ENZ wavelength, as the modes merge leading to a higher FE.

The E_y field is directly proportional to the permittivity of the incident medium (i.e. 25), which is one of the reasons why our FE values are high. To further confirm the existence of the hybrid mode, we present the field distribution plots displaying the ENZ mode, the SPR mode, and their co-existence, given the

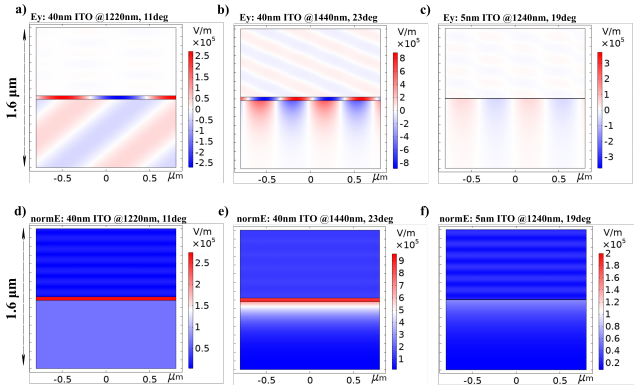

Fig. 3. Field distribution in the computational domain (configuration 1) observed at the ENZ and SPR wavelengths (a-b) (d-e) E_y field and electric field norm observed at ENZ and SPR mode conditions, (c-f) E_y field and the electric field norm observed at the hybrid mode conditions.

right conditions. Here, Figs. 3(a-b), (d-e) show the E_y and the electric field norm distribution for a 40 nm thick ITO layer at the wavelengths corresponding to the hotspots found in Fig. 2. Fig. 3(a) shows the ENZ mode with the field mostly confined inside the material, while Fig. 3(b) illustrates the propagating plasmon-polariton mode. Here, both the modes showcase high FE inside the ITO layer. However, the SPP mode contains a surface wave that can be observed in Fig. 3(b). The electric field norm plots (Figs. 3(d-f)) of the corresponding ENZ and SPP modes illustrate a high FE in the ITO layer and an additional FE for the SPP mode at the ITO layer-substrate interface. The plots correspond to the hotspots at different wavelengths and incident angles. In Fig. 3(d), the field is concentrated inside the material, and in Fig. 3(e), enhancement is seen both inside as well as outside the ITO layer as it is a surface wave. Now, as we reduce the thickness, the modes merge, bringing out the best of both worlds. In a 5 nm thick ITO layer, we can see a surface wave coupled with the confined ENZ mode. Fig. 3(c) shows a week SPP mode coupled to the ENZ mode, and its corresponding electric field norm plot depicts a FE similar to SPP mode but at ENZ wavelengths, indicating the merging of modes. The coupling results in an increase in field enhancement (E_y). This combination is what we call the hybrid mode.

B. Configuration 2

To observe the hybrid mode in a more practical scenario, we used a grating configuration. Here, the ITO layer is in the form of a sinusoidal grating. When light is incident on the ITO layer, diffraction from the grating assists with the momentum matching and thereby excites a plasmon. Unlike the configuration 1, the incident medium has an easily achievable relative permittivity, i.e., 1. The substrate, on which the grating rests, has a permittivity of 2.25. We chose a sinusoidal grating with a period of 1.7 μm, and the boundary conditions are adapted from the previous configuration.

We collected the results by varying the thickness of the grating. The ENZ enhancement remains at the same wavelength, even though the ITO layer is not flat but in a curved grating form. The FE is confined to the grating layer and can be observed for a wide range of incidence angles. However, the location and the nature of SPR changes in this case. Here, the plasmons are observed at the air-ITO layer interface. The FE plots in Figs.

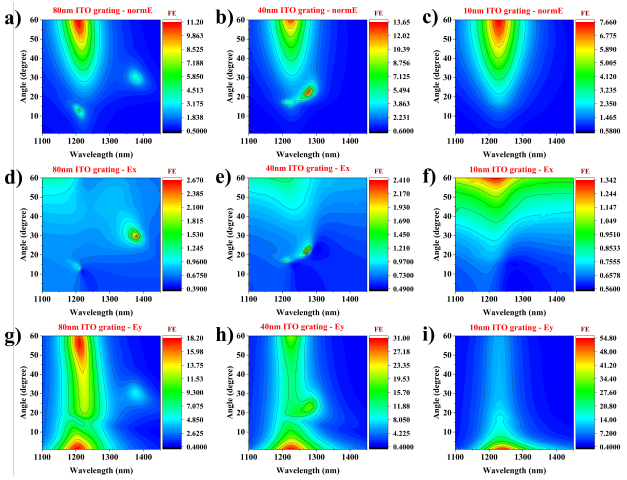

Fig. 4. Field enhancement (FE) plots vs. wavelength and the angle of incidence, observed in the configuration 2 by varying the thickness of ITO grating deposited on a dielectric of RI 1.5 (a-c) Electric field norm, (d-f) E_x field related FE, and (g-i) E_y field enhancement.

4 follow the same notable trend we observed in Figs. 2. We do observe two localized hotspots, when the grating is thick ($> 20nm$), and they merge into one as the thickness approaches 10nm. There is an increase in the FE value from 9.8 to 14.8 in the E_y field case, as shown in Figs. 4(g-i). This increase is a result of a reduction in the thickness that results in the merging of SPR enhancement. However, E_x FE follows a different trend. This effect could be due to the weak plasmon excitation. For a perfectly coupled surface wave, one can observe a dip in the reflectivity plot. As we reduce the thickness, reflectivity increases leading to a weak surface wave. We in fact see the same behavior in our system, where a weak surface wave is generated as the thickness reduces. E_x FE plots in Figs. 4(d-f) demonstrate the same. The electric field norm, which is a resultant of E_x and E_y FE plots, also assumes the same trend of E_x. Another similarity with respect to the results of the Kretschmann configuration is the shift in the angle of incidence. The angle gradually reduces and merges with the ENZ enhancement. However, the ENZ enhancement here is located at the ENZ wavelength and spreads over various angles of incidence. This expansion could be a result of the momentum matching by different diffraction orders (they can either add up or subtract) at various incidence angles. Our further parametric analysis on the variation of RI of ITO substrate and its grating period is enclosed in the Supplementary file.

In conclusion, we put forth the theory of a hybrid mode, the point where the long-range plasmon mode dispersion curve intersects with the ENZ dispersion curve. With the help of numerical simulations, we illustrated the existence of this mode. We performed parametric analysis on two arrangements - Kretschmann and grating configurations. Both configurations allow for the intersection of SPP and ENZ modes upon varying the thickness of the ITO layer. As the thickness of the ITO layer reduces, the LRP curve shifts towards the ENZ flat-line dispersion. However, the grating configuration is more feasible to implement experimentally , as it does not require a high RI incident medium. We performed further analysis by varying the ITO substrate permittivity to understand the effect on the shift of LRP towards the ENZ curve. After determining the existence of the hybrid mode, we made efforts to optimize the grating period with the help of analytical equations. Our numerical results agree with the assumptions, and we illustrated the same with the help of 2D contour plots. This work provides detailed understanding of how the hybrid ENZ/SPP mode can be excited and manipulated to produce the extremely high local field for various applications in nonlinear photonics, including highly efficient frequency up-converting materials.

Funding. Defense Advanced Research Projects Agency (D19AC0017)

Disclosures. The authors declare no conflicts of interest.

See Supplement file for additional parametric analysis

REFERENCES

1. A. Baev, P. N. Prasad, H. Agren, M. Samoc, and M. Wegener, Phys. Reports-Review Sect. Phys. Lett. **594**, 1 (2015).
2. A. Alu, M. G. Silveirinha, A. Salandrino, and N. Engheta, Phys. Rev. B **75** (2007).
3. M. Z. Alam, I. De Leon, and R. W. Boyd, Science **352**, 795 (2016).
4. A. Capretti, Y. Wang, N. Engheta, and L. Dal Negro, Acs Photonics **2**, 1584 (2015).
5. J. Kyoung, D. J. Park, S. J. Byun, J. Lee, S. B. Choi, S. Park, and S. W. Hwang, Opt. Express **22**, 31875 (2014).
6. M. Silveirinha and N. Engheta, Phys. Rev. Lett. **97** (2006).
7. S. Vassant, A. Archambault, F. Marquier, F. Pardo, U. Gennser, A. Cavanna, J. L. Pelouard, and J. J. Greffet, Phys. Rev. Lett. **109** (2012).
8. S. Vassant, J. P. Hugonin, F. Marquier, and J. J. Greffet, Opt. Express **20**, 23971 (2012).
9. D. W. Berreman, Phys. Rev. **130**, 2193 (1963).
10. B. Harbecke, B. Heinz, and P. Grosse, Appl. Phys. a-Materials Sci. & Process. **38**, 263 (1985).
11. S. Campione, D. de Ceglia, M. A. Vincenti, M. Scalora, and F. Capolino, Phys. Rev. B **87** (2013).
12. S. Campione, I. Brener, and F. Marquier, Phys. Rev. B **91** (2015).
13. E. N. Economou, Phys. Rev. **182**, 539 (1969).
14. S. Campione, I. Kim, D. de Ceglia, G. A. Keeler, and T. S. Luk, Opt. Express **24**, 18782 (2016).
15. T. Taliercio, V. N. Guilengui, L. Cerutti, E. Tournic, and J. J. Greffet, Opt. Express **22**, 24294 (2014).
16. J. Luo, S. C. Li, B. Hou, and Y. Lai, Phys. Rev. B **90** (2014).
17. S. M. Zhong, Y. G. Ma, and S. L. He, Appl. Phys. Lett. **105** (2014).
18. S. Vassant, J. P. Hugonin, and J. J. Greffet, Opt. Express **27**, 12317 (2019).
19. E. L. Runnerstrom, K. P. Kelley, T. G. Folland, J. R. Nolen, N. Engheta, J. D. Caldwell, and J. P. Maria, Nano Lett. **19**, 948 (2019).
20. G. Subramania, A. J. Fischer, and T. S. Luk, Appl. Phys. Lett. **101** (2012).
21. M. J. Roberts, S. M. Feng, M. Moran, and L. Johnson, J. Nanophotonics **4** (2010).
22. J. Gao, L. Sun, H. X. Deng, C. J. Mathai, S. Gangopadhyay, and X. D. Yang, Appl. Phys. Lett. **103** (2013).
23. C. Rizza, X. Li, A. Di Falco, E. Palange, A. Marini, and A. Ciattoni, J. Opt. **20** (2018).
24. N. Kinsey and J. Khurgin, Opt. Mater. Express **9**, 2793 (2019).
25. X. Li, C. Pizza, S. A. Schulz, A. Ciattoni, and A. Di Falco, Apl Photonics **4** (2019).
26. P. Berini, Adv. Opt. Photonics **1**, 484 (2009).
27. C. Rhodes, S. Franzen, J. P. Maria, M. Losego, D. N. Leonard, B. Laughlin, G. Duscher, and S. Weibel, J. Appl. Phys. **100** (2006).
28. B. Szabó and I. Babuška, *Finite element analysis* (John Wiley & Sons, 1991).
29. T. A. Bither, R. J. Bouchard, W. H. Cloud, P. C. Donohue, and W. J. Siemons, Inorg. Chem. **7**, 2208 (1968).
30. A. J. J. Che, L. F. Drummy, J. Bultman, A. Waite, M. S. Hsiao, and R. A. Vaia, Acs Nano **11**, 635 (2017).

FULL REFERENCES

1. A. Baev, P. N. Prasad, H. Agren, M. Samoc, and M. Wegener, "Metaphotonics: An emerging field with opportunities and challenges," Phys. Reports-Review Sect. Phys. Lett. **594**, 1–60 (2015).
2. A. Alu, M. G. Silveirinha, A. Salandrino, and N. Engheta, "Epsilon-near-zero metamaterials and electromagnetic sources: Tailoring the radiation phase pattern," Phys. Rev. B **75** (2007).
3. M. Z. Alam, I. De Leon, and R. W. Boyd, "Large optical nonlinearity of indium tin oxide in its epsilon-near-zero region," Science **352**, 795–797 (2016).
4. A. Capretti, Y. Wang, N. Engheta, and L. Dal Negro, "Comparative study of second-harmonic generation from epsilon-near-zero indium tin oxide and titanium nitride nanolayers excited in the near-infrared spectral range," Acs Photonics **2**, 1584–1591 (2015).
5. J. Kyoung, D. J. Park, S. J. Byun, J. Lee, S. B. Choi, S. Park, and S. W. Hwang, "Epsilon-near-zero meta-lens for high resolution wide-field imaging," Opt. Express **22**, 31875–31883 (2014).
6. M. Silveirinha and N. Engheta, "Tunneling of electromagnetic energy through subwavelength channels and bends using epsilon-near-zero materials," Phys. Rev. Lett. **97** (2006).
7. S. Vassant, A. Archambault, F. Marquier, F. Pardo, U. Gennser, A. Cavanna, J. L. Pelouard, and J. J. Greffet, "Epsilon-near-zero mode for active optoelectronic devices," Phys. Rev. Lett. **109** (2012).
8. S. Vassant, J. P. Hugonin, F. Marquier, and J. J. Greffet, "Berreman mode and epsilon near zero mode," Opt. Express **20**, 23971–23977 (2012).
9. D. W. Berreman, "Infrared absorption at longitudinal optic frequency in cubic crystal films," Phys. Rev. **130**, 2193–& (1963).
10. B. Harbecke, B. Heinz, and P. Grosse, "Optical-properties of thin-films and the berreman effect," Appl. Phys. a-Materials Sci. & Process. **38**, 263–267 (1985).
11. S. Campione, D. de Ceglia, M. A. Vincenti, M. Scalora, and F. Capolino, "Electric field enhancement in epsilon-near-zero slabs under tm-polarized oblique incidence," Phys. Rev. B **87** (2013).
12. S. Campione, I. Brener, and F. Marquier, "Theory of epsilon-near-zero modes in ultrathin films," Phys. Rev. B **91** (2015).
13. E. N. Economou, "Surface plasmons in thin films," Phys. Rev. **182**, 539–& (1969).
14. S. Campione, I. Kim, D. de Ceglia, G. A. Keeler, and T. S. Luk, "Experimental verification of epsilon-near-zero plasmon polariton modes in degenerately doped semiconductor nanolayers," Opt. Express **24**, 18782–18789 (2016).
15. T. Taliercio, V. N. Guilengui, L. Cerutti, E. Tournic, and J. J. Greffet, "Brewster "mode" in highly doped semiconductor layers: an all-optical technique to monitor doping concentration," Opt. Express **22**, 24294–24303 (2014).
16. J. Luo, S. C. Li, B. Hou, and Y. Lai, "Unified theory for perfect absorption in ultrathin absorptive films with constant tangential electric or magnetic fields," Phys. Rev. B **90** (2014).
17. S. M. Zhong, Y. G. Ma, and S. L. He, "Perfect absorption in ultrathin anisotropic epsilon-near-zero metamaterials," Appl. Phys. Lett. **105** (2014).
18. S. Vassant, J. P. Hugonin, and J. J. Greffet, "Quasi-confined enz mode in an anisotropic uniaxial thin slab," Opt. Express **27**, 12317–12335 (2019).
19. E. L. Runnerstrom, K. P. Kelley, T. G. Folland, J. R. Nolen, N. Engheta, J. D. Caldwell, and J. P. Maria, "Polaritonic hybrid-epsilon-near-zero modes: Beating the plasmonic confinement vs propagation-length trade-off with doped cadmium oxide bilayers," Nano Lett. **19**, 948–957 (2019).
20. G. Subramania, A. J. Fischer, and T. S. Luk, "Optical properties of metal-dielectric based epsilon near zero metamaterials," Appl. Phys. Lett. **101** (2012).
21. M. J. Roberts, S. M. Feng, M. Moran, and L. Johnson, "Effective permittivity near zero in nanolaminates of silver and amorphous polycarbonate," J. Nanophotonics **4** (2010).
22. J. Gao, L. Sun, H. X. Deng, C. J. Mathai, S. Gangopadhyay, and X. D. Yang, "Experimental realization of epsilon-near-zero metamaterial slabs with metal-dielectric multilayers," Appl. Phys. Lett. **103** (2013).
23. C. Rizza, X. Li, A. Di Falco, E. Palange, A. Marini, and A. Ciattoni, "Enhanced asymmetric transmission in hyperbolic epsilon-near-zero slabs," J. Opt. **20** (2018).
24. N. Kinsey and J. Khurgin, "Nonlinear epsilon-near-zero materials explained: opinion," Opt. Mater. Express **9**, 2793–2796 (2019).
25. X. Li, C. Pizza, S. A. Schulz, A. Ciattoni, and A. Di Falco, "Conformable optical coatings with epsilon near zero response," Apl Photonics **4** (2019).
26. P. Berini, "Long-range surface plasmon polaritons," Adv. Opt. Photonics **1**, 484–588 (2009).
27. C. Rhodes, S. Franzen, J. P. Maria, M. Losego, D. N. Leonard, B. Laughlin, G. Duscher, and S. Weibel, "Surface plasmon resonance in conducting metal oxides," J. Appl. Phys. **100** (2006).
28. B. Szabó and I. Babuška, *Finite element analysis* (John Wiley & Sons, 1991).
29. T. A. Bither, R. J. Bouchard, W. H. Cloud, P. C. Donohue, and W. J. Siemons, "Transition metal pyrite dichalcogenides high-pressure synthesis and correlation of properties," Inorg. Chem. **7**, 2208–& (1968).
30. A. J. J. Che, L. F. Drummy, J. Bultman, A. Waite, M. S. Hsiao, and R. A. Vaia, "Redox exfoliation of layered transition metal dichalcogenides," Acs Nano **11**, 635–646 (2017).